Electronic Supplementary Material (ESI) for Inorganic Chemistry Frontiers.

Supporting Information

pH-Responsive Iridium(III) Two-Photon Photosensitizer Loaded $CaCO_3$ Nanoplatform for Combined Ca^{2+} Overload and Photodynamic Therapy

Jinchao Shen,[a‡] Xinxing Liao,[a‡] Weijun Wu,[a‡] Tao Feng,[a] Johannes Karges,[b] Mingwei Lin,[a] Hongjie Luo,[a] Yu Chen,[a] Hui Chao[a,c]*

[a] *MOE Key Laboratory of Bioinorganic and Synthetic Chemistry, School of Chemistry, Guangdong Provincial Key Laboratory of Digestive Cancer Research, The Seventh Affiliated Hospital, Sun Yat-Sen University, Guangzhou, 510006, P. R. China*
[b] *Department of Chemistry and Biochemistry, University of California, San Diego, 9500 Gilman Drive, La Jolla, CA 92093, United States.*
[c] *MOE Key Laboratory of Theoretical Organic Chemistry and Functional Molecule, School of Chemistry and Chemical Engineering, Hunan University of Science and Technology, Xiangtan, 400201, P. R. China*

* Corresponding author: ceschh@mail.sysu.edu.cn (H. Chao)

Table of contents

FIGURES AND TABLE

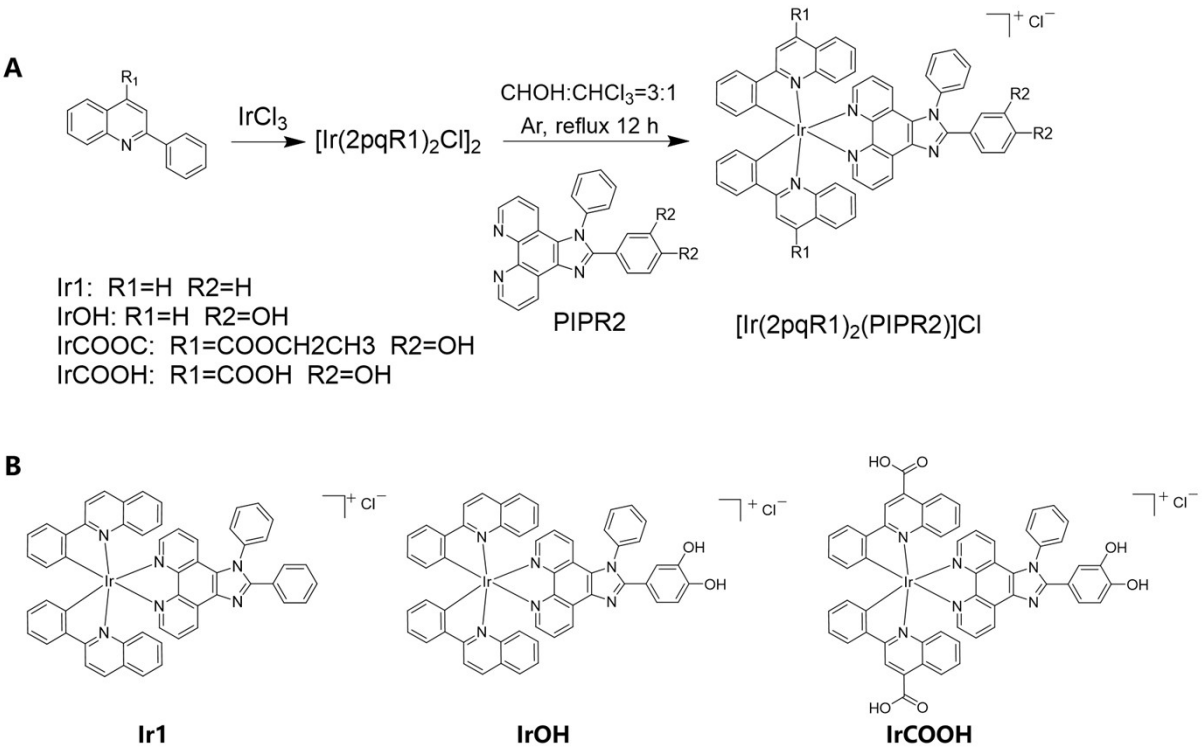

Figure S1. Synthesis strategy and structure of **Ir1**, **IrOH**, and **IrCOOH**.

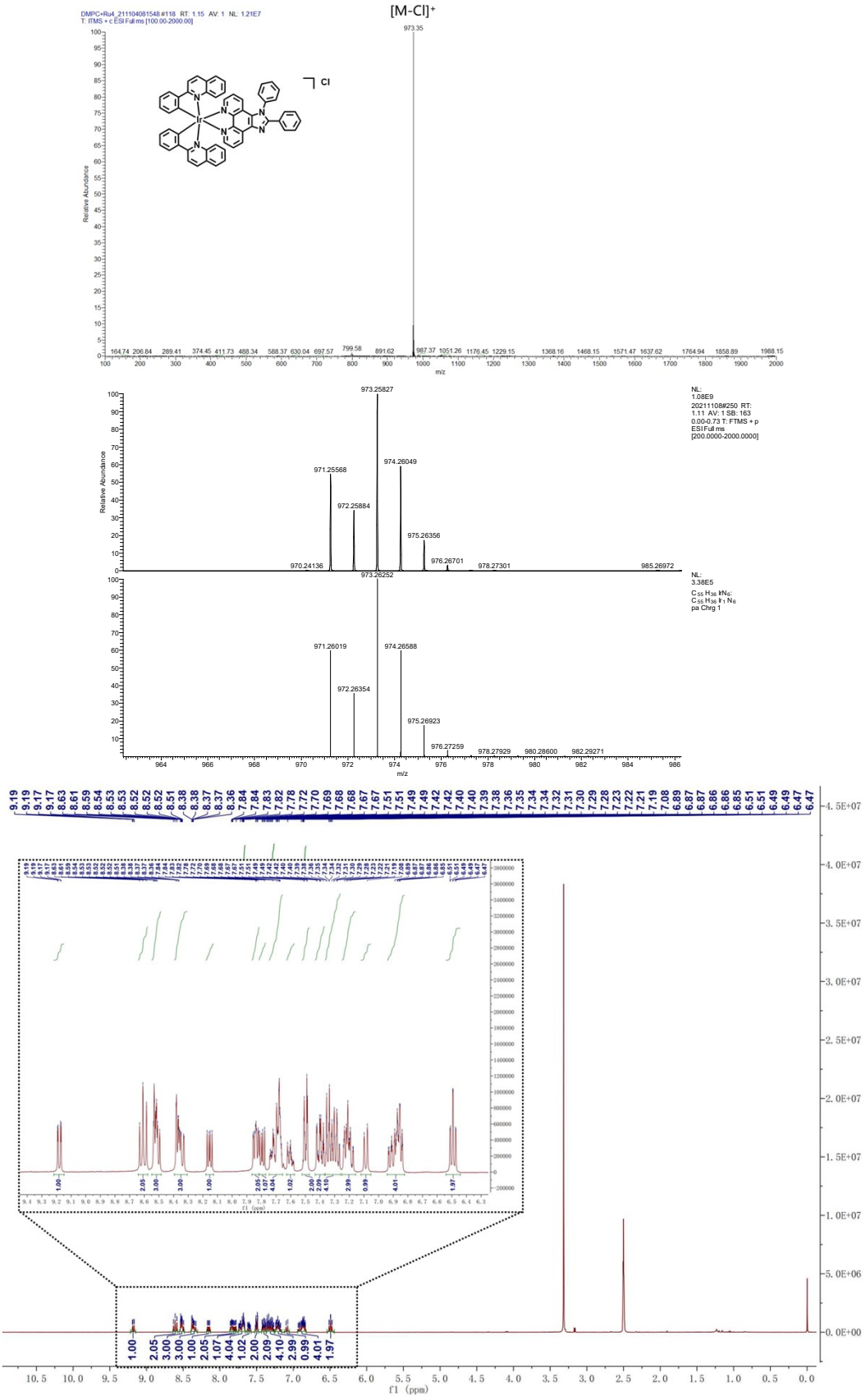

Figure S2. ESI-MS, HR-ESI-MS, and ^{1}H-NMR spectra of **Ir1**.

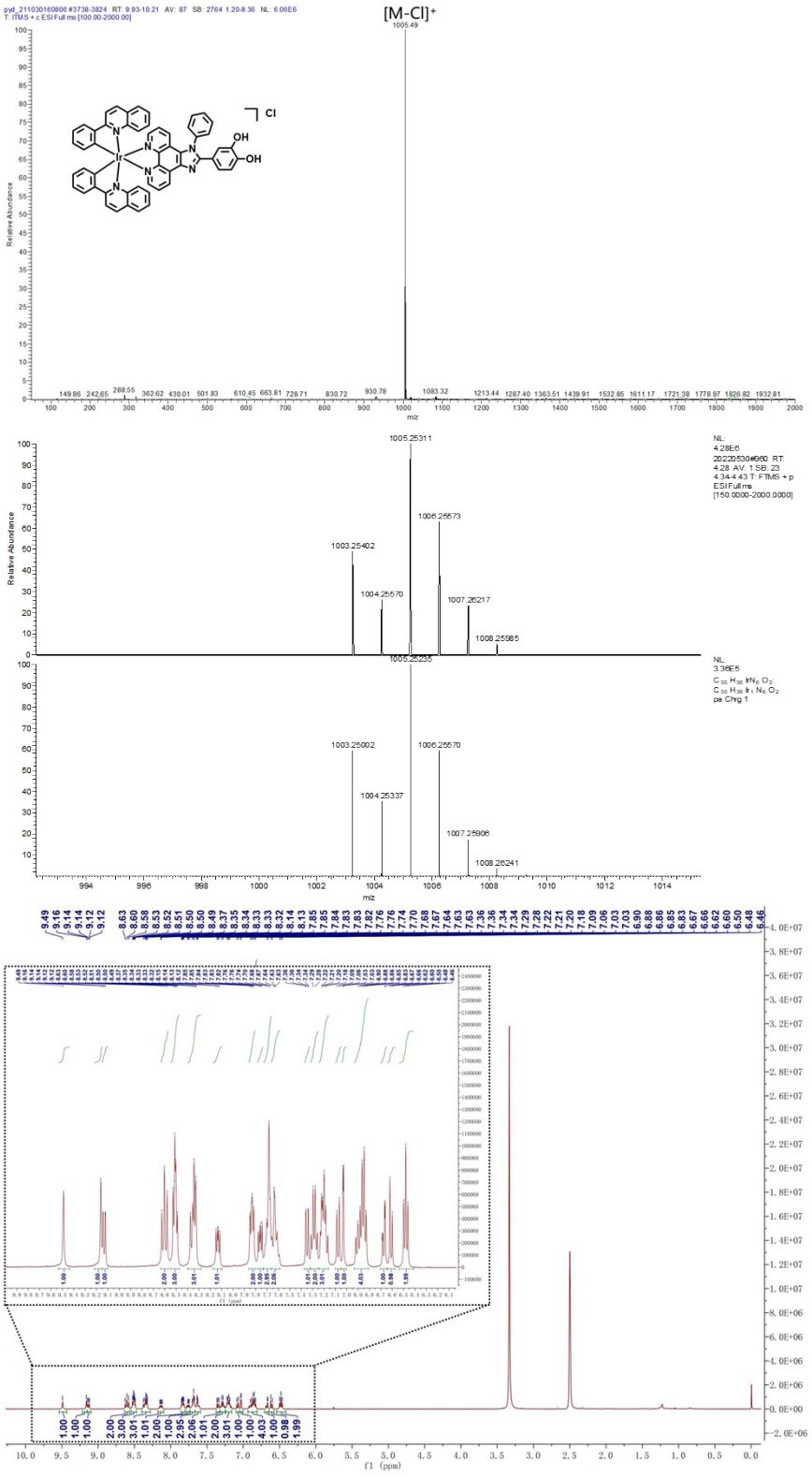

Figure S3. ESI-MS, HR-ESI-MS, and ^{1}H-NMR spectra of **IrOH**.

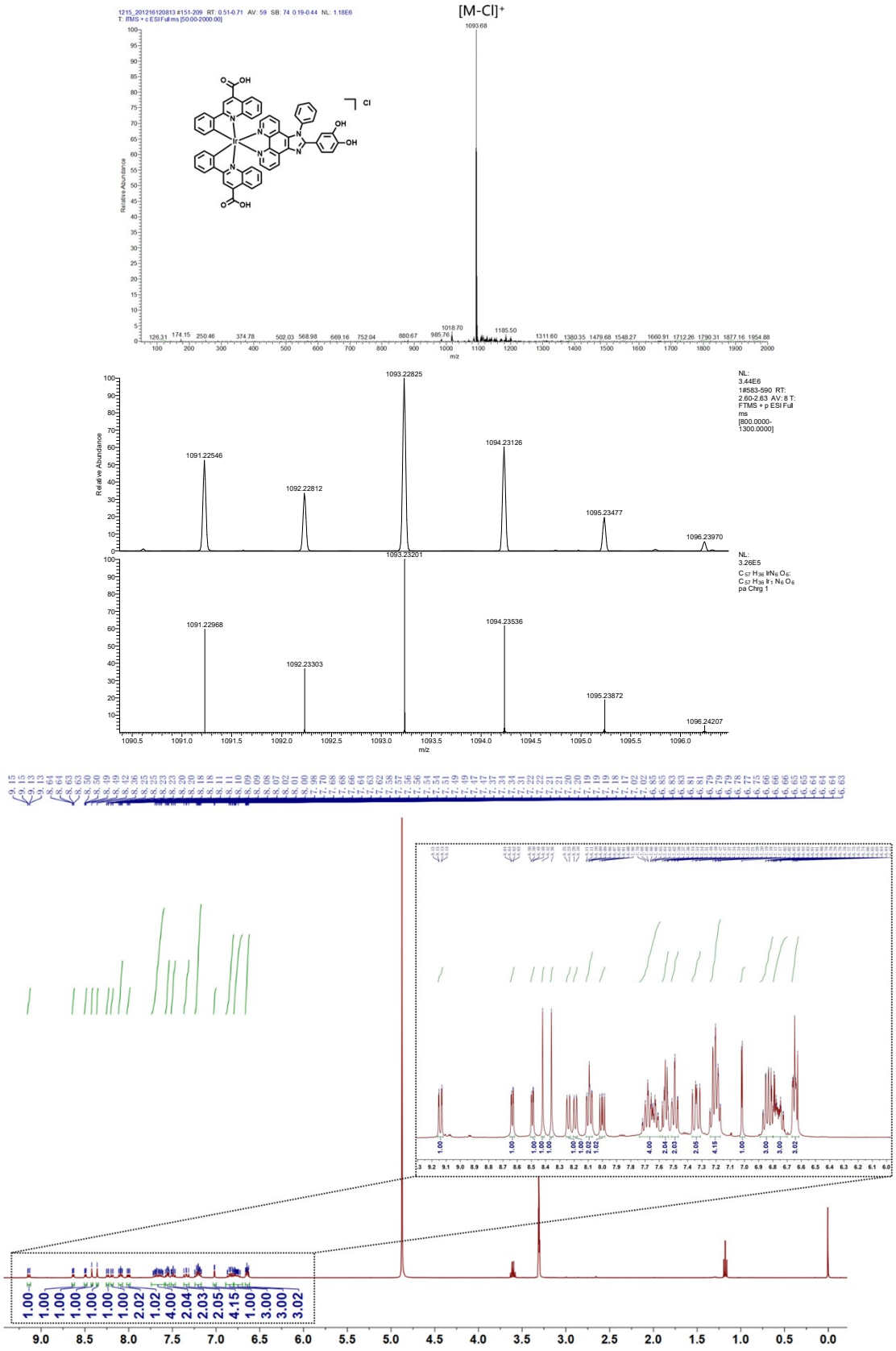

Figure S4. ESI-MS, HR-ESI-MS, and ^{1}H-NMR spectra of **IrCOOH**.

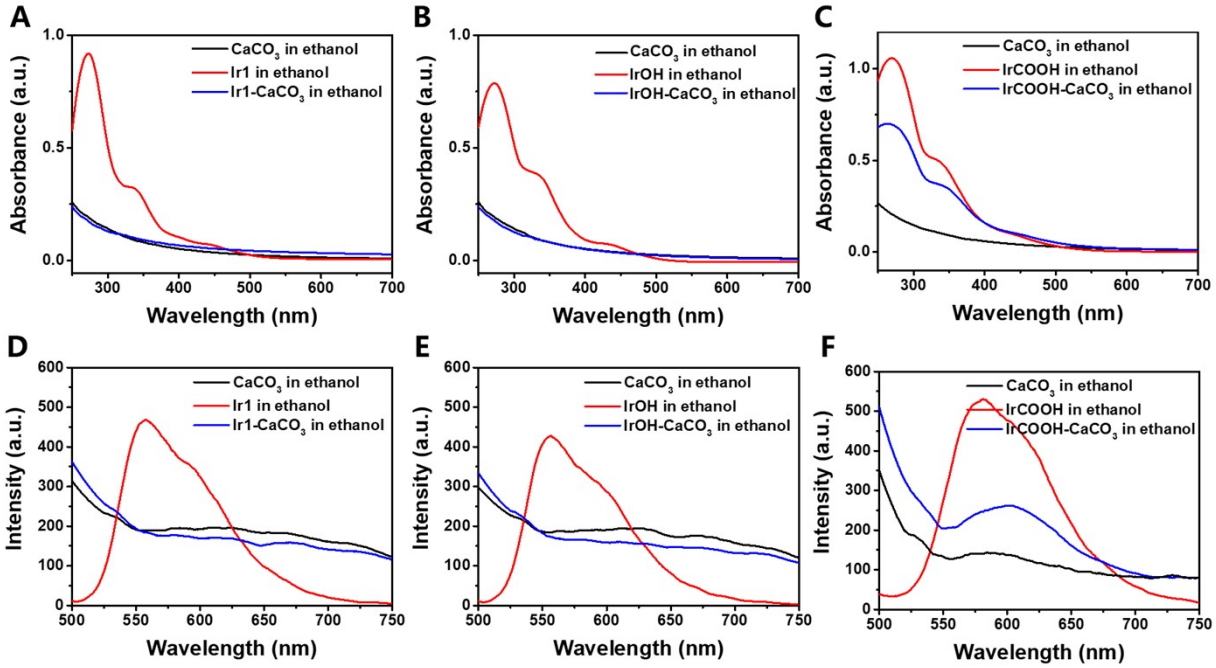

Figure S5. Absorption (A, B, C) and emission spectra (D, E, F) of $CaCO_3$ nanocarriers loaded with the respective Ir(III) complexes.

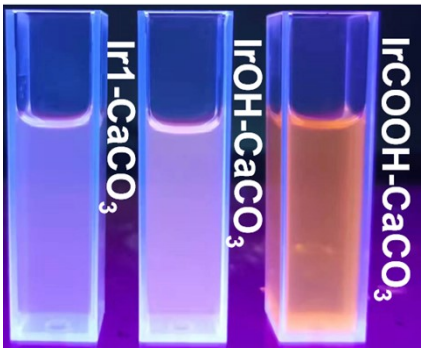

Figure S6. Photographs of **Ir1-$CaCO_3$**, **IrOH-$CaCO_3$**, **IrCOOH-$CaCO_3$** upon UV irradiation.

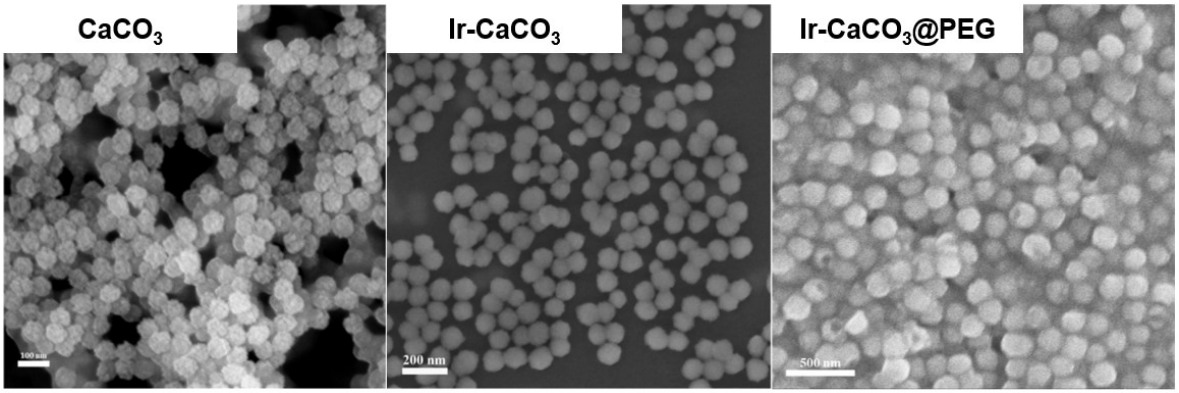

Figure S7. SEM images of **$CaCO_3$**, **Ir-$CaCO_3$**, and **Ir-$CaCO_3$@PEG** nanoparticles.

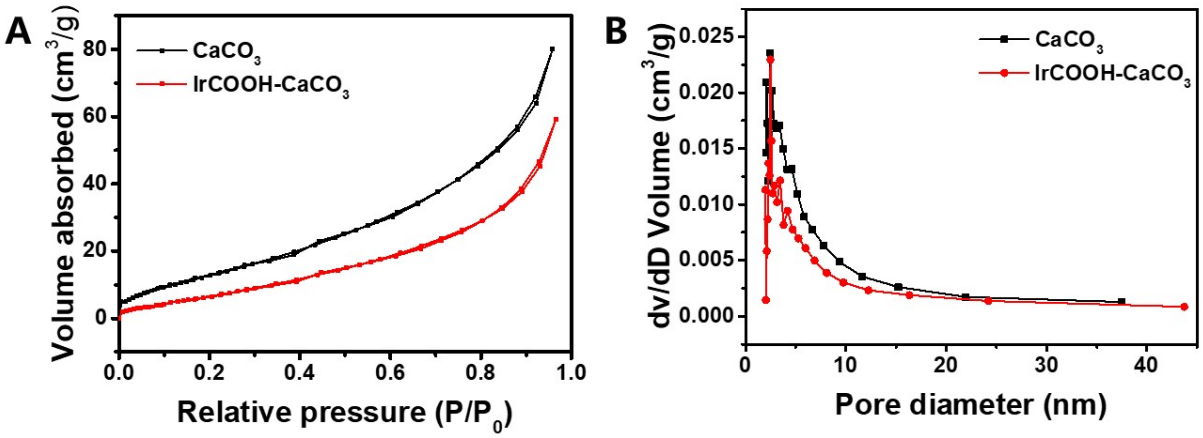

Figure S8. Barrett-Joyner-Halenda (BJH) pore size and Bunauer-Emmett-Teller (BET) surface area analyses.

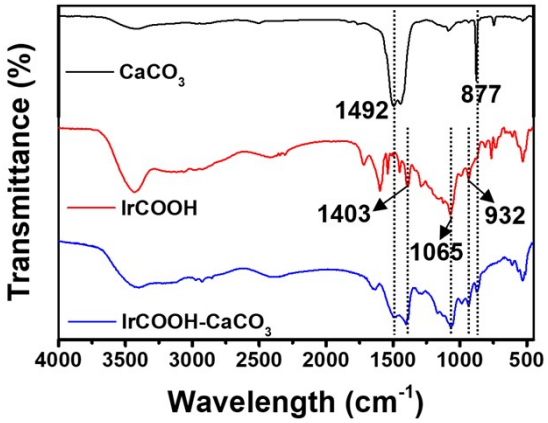

Figure S9. FT-IR spectrum of **$CaCO_3$**, **IrCOOH**, and **IrCOOH-$CaCO_3$**.

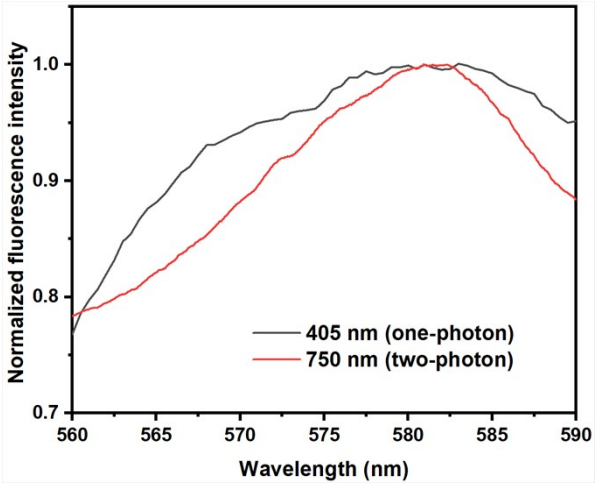

Figure S10. The overlap of the **IrCOOH** emission spectra upon one and two-photon excitation.

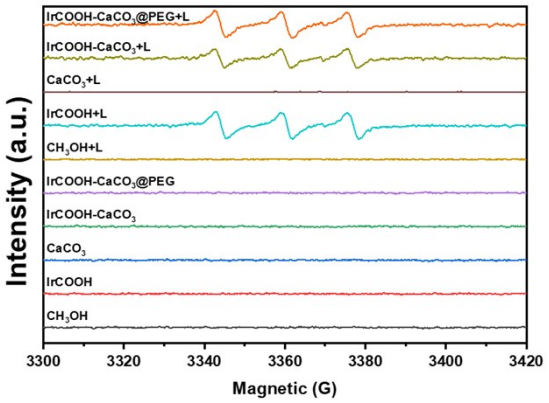

Figure S11. Electron spin resonance spectrum of the respective compound with the singlet oxygen scavenger 2,2,6,6-tetramethylpiperidine in the dark or upon two-photon laser irradiation (750 nm, 50 mW, 300 s).

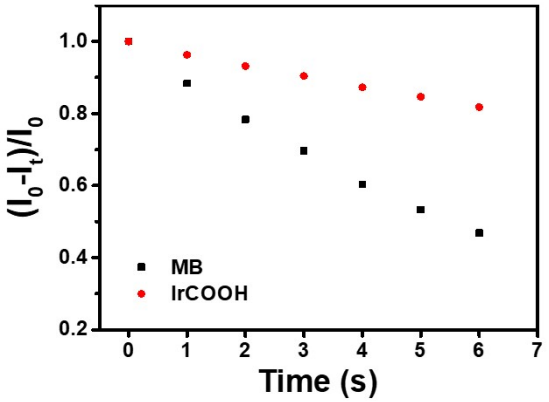

Figure S12. Change in absorbance of the singlet oxygen scavenger 1,3-diphenylisobenzofuran upon incubation with methylene blue (MB) or **IrCOOH** and irradiation at 405 nm in methanol in various time intervals.

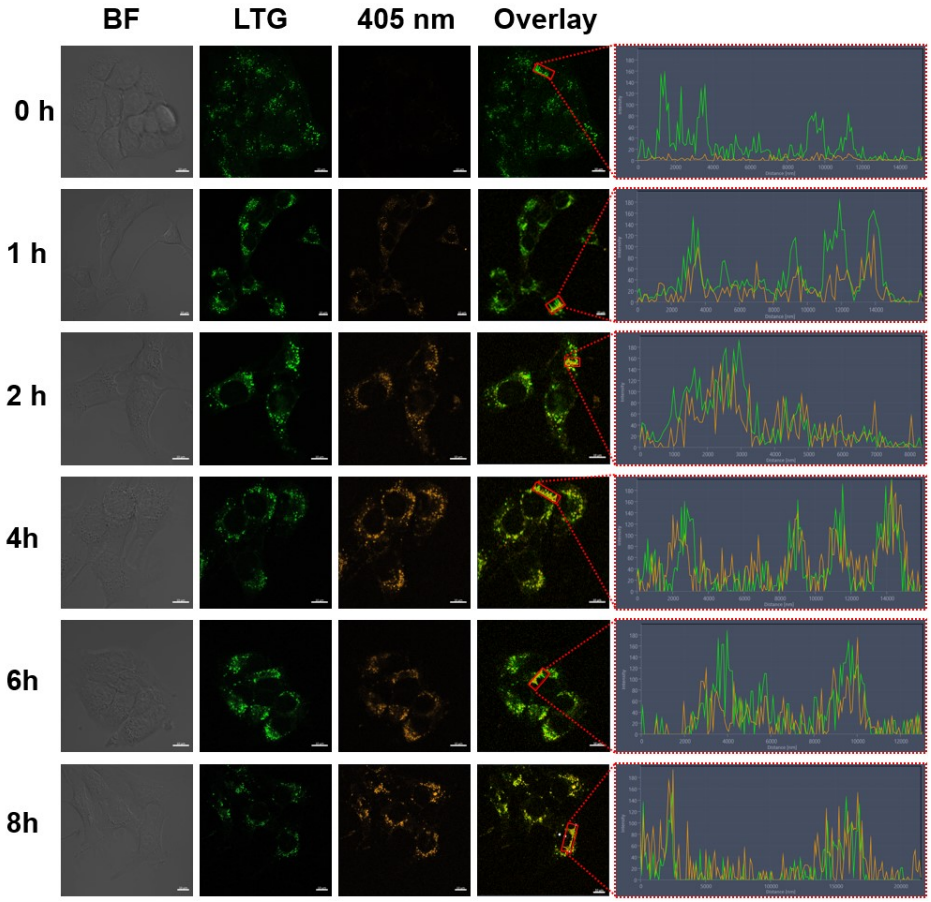

Figure S13. Confocal laser scanning microscopy images and corresponding colocalization of 4T1 cells incubated with **IrCOOH-$CaCO_3$@PEG** (λex = 405 nm, λem = 580 - 600 nm) as well as LysoTracker™ Green DND-26 (LTG) (λex = 488 nm, λem = 500 - 520 nm) at different time points. Scale bar = 10 μm.

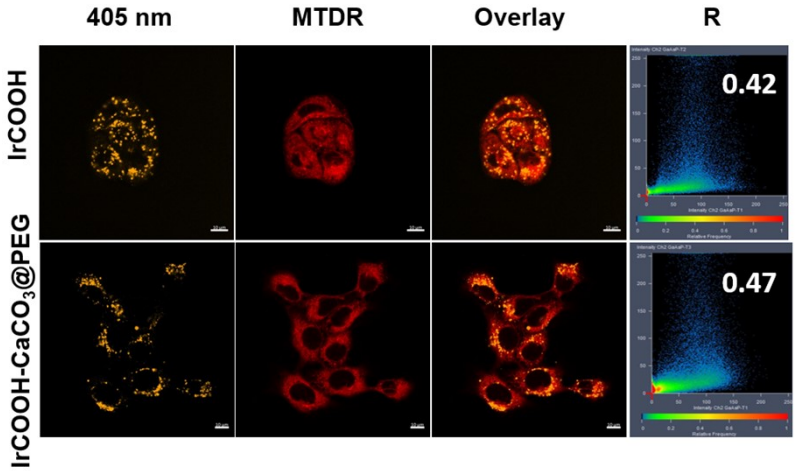

Figure S14. Confocal laser scanning microscopy images and corresponding colocalization coefficient (R) of 4T1 cells incubated with **IrCOOH** or **IrCOOH-$CaCO_3$@PEG** (λ_{ex} = 405 nm, λ_{em} = 580 - 600 nm) as well as Mito Tracker Deep Red (MTDR) (λ_{ex} = 644 nm, λ_{em} = 650 - 670 nm). Scale bar = 20 μm.

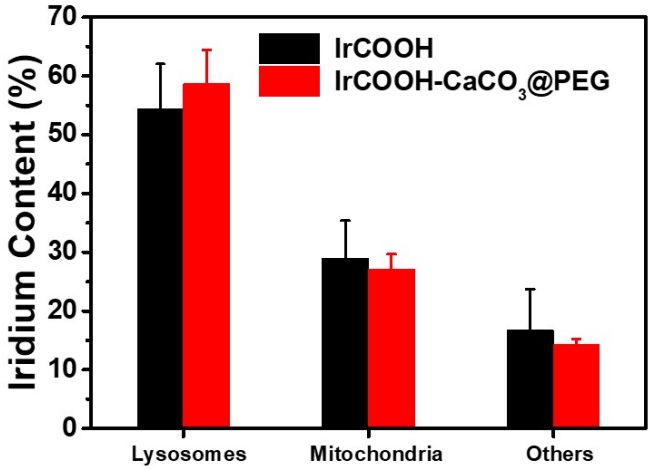

Figure S15. Subcellular distribution of **IrCOOH** or **IrCOOH-$CaCO_3$@PEG** is determined by inductively coupled plasma mass spectrometry upon incubation for 8 h.

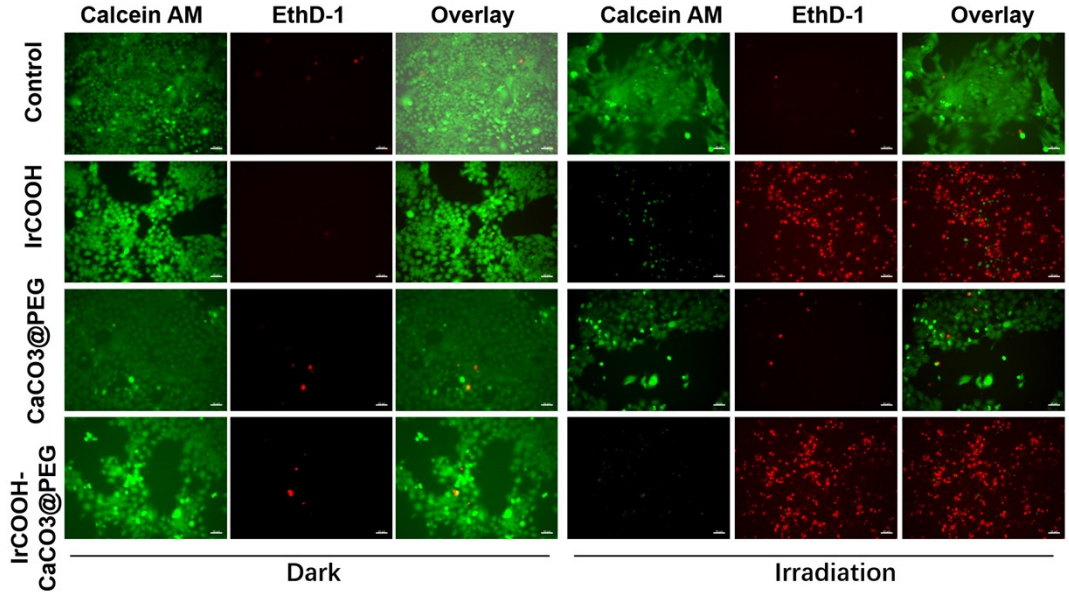

Figure S16. Confocal laser scanning microscopy images of 4T1 cells incubated with **IrCOOH**, **$CaCO_3$@PEG**, or **IrCOOH-$CaCO_3$@PEG** in the dark or upon 405 nm laser irradiation (12 J cm^{-2}), followed by staining with Calcein-AM/EthD-1 (Calcein-AM for live cells: λ_{ex} = 488 nm, λ_{em} = 500-520 nm; EthD-1 for dead cells: λ_{ex} = 543 nm, λ_{em} = 590 - 630 nm). Scale bar = 50 μm.

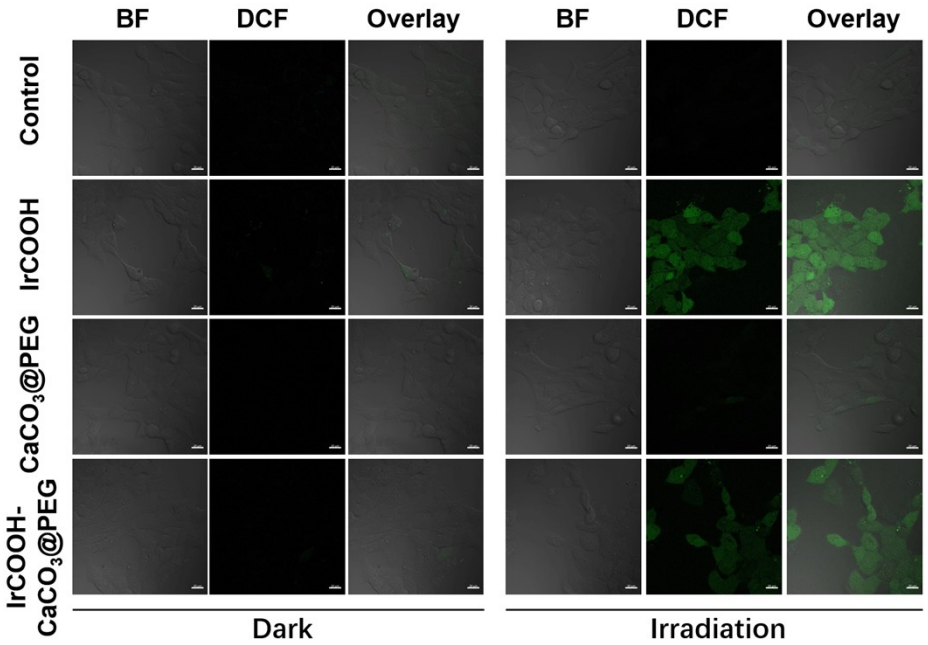

Figure S17. Confocal laser scanning microscopy images of 4T1 cells incubated with different materials and stained with 2,7-dichlorodihydrofluorescein (λ_{ex} = 488 nm, λ_{em} = 500-520 nm) in the dark or upon 405 nm irradiation. Scale bar = 50 μm.

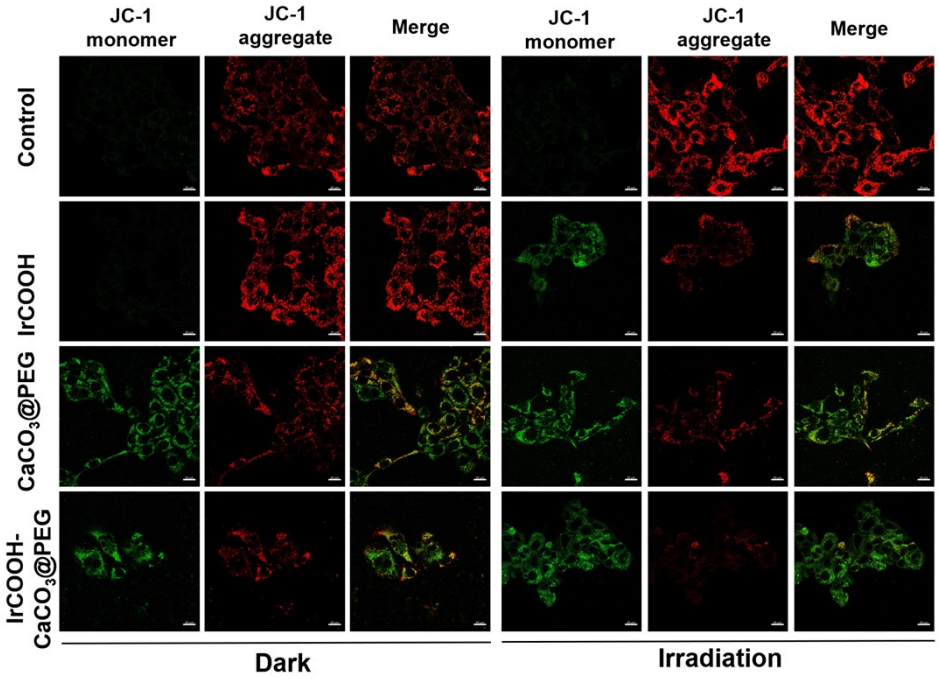

Figure S18. Confocal laser scanning microscopy images of 4T1 cells incubated with the specific mitochondrial membrane potential dye JC-1 and treated with different materials in the dark or upon 405 nm irradiation. Monomer: λ_{ex} = 488 nm, λ_{em} = 500-520 nm; Aggregates: λ_{ex} = 543 nm, λ_{em} = 590-630 nm. Scale bar = 20 μm.

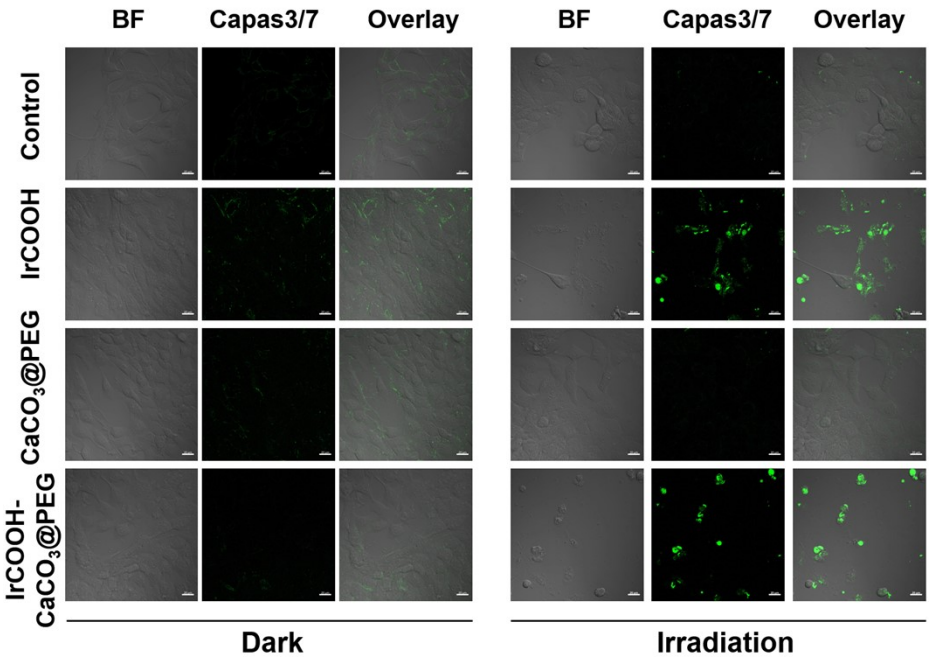

Figure S19. Confocal laser scanning microscopy images of 4T1 cells incubated with the specific caspase 3/7 dye and treated with different materials in the dark or upon 405 nm irradiation. λ_{ex} = 488 nm, λ_{em} = 500-520 nm. Scale bar = 50 μm.

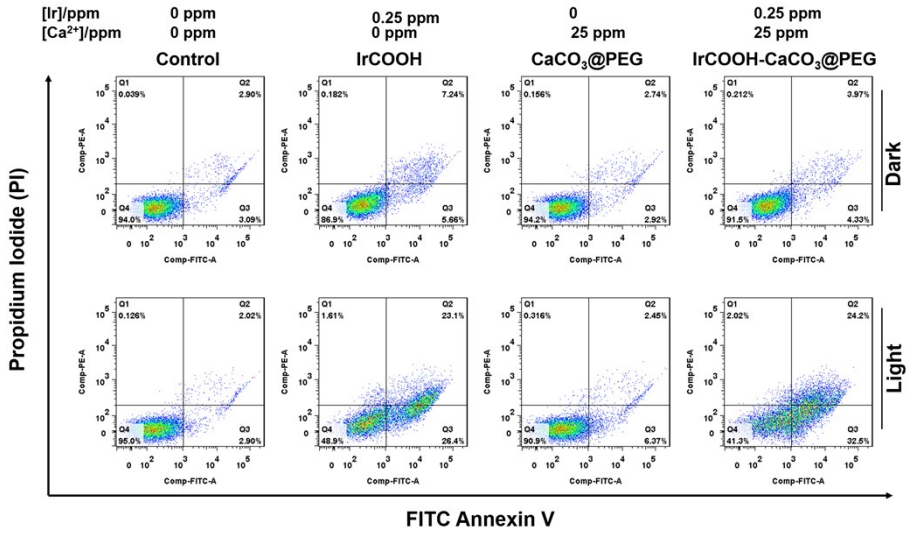

Figure S20. Flow-cytometry assay of Annexin-FITC/PI stained 4T1 cells incubated with different materials in the dark or upon 405 nm irradiation.

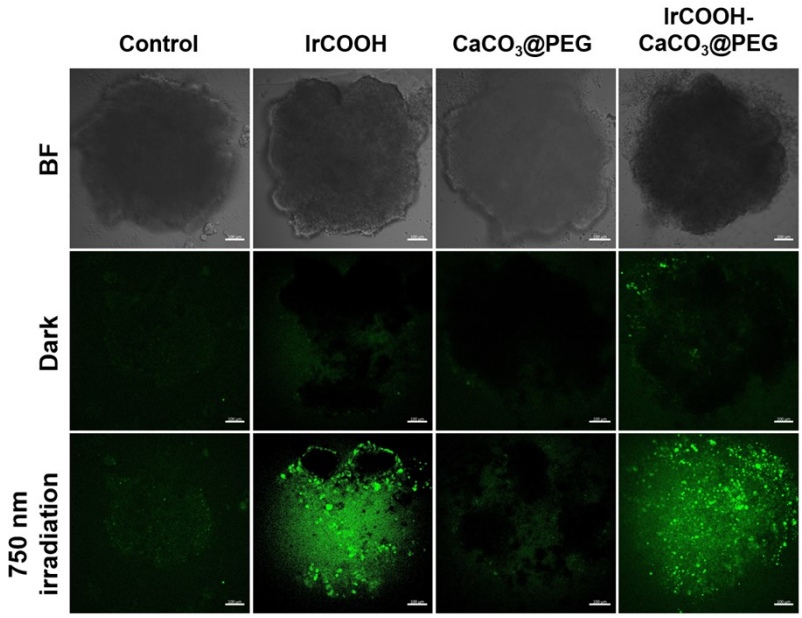

Figure S21. Confocal laser scanning microscopy images of 4T1 3D multicellular tumour spheroid incubated with different materials and stained with 2,7-dichlorodihydrofluorescein (λ_{ex} = 488 nm, λ_{em} = 500-520 nm) in the dark or upon 750 nm irradiation. Scale bar = 100 μm.

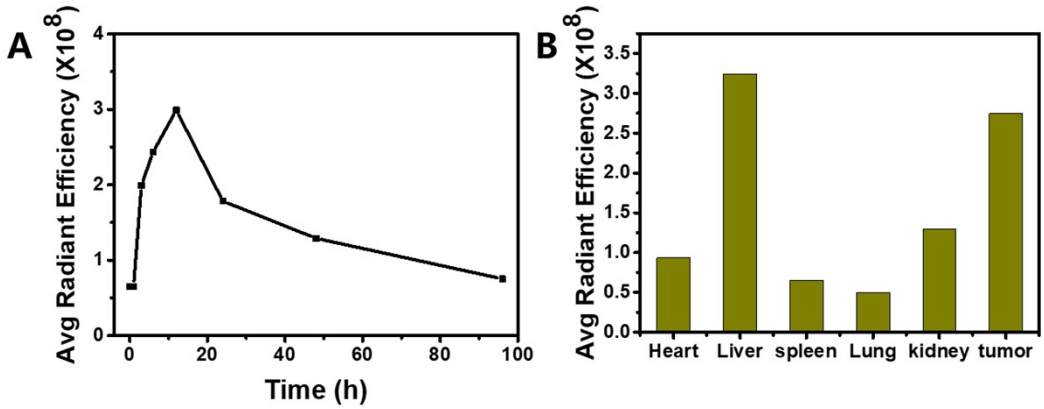

Figure S22. (A) Time-dependent observation of the luminescence signal at the tumor site after intravenous injection. (B) Average luminescence within the tumor and main organs 12 h after intravenous injection.

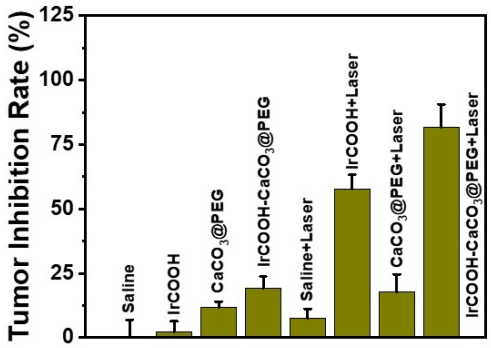

Figure S23. Tumor-inhibition rate after various treatments.

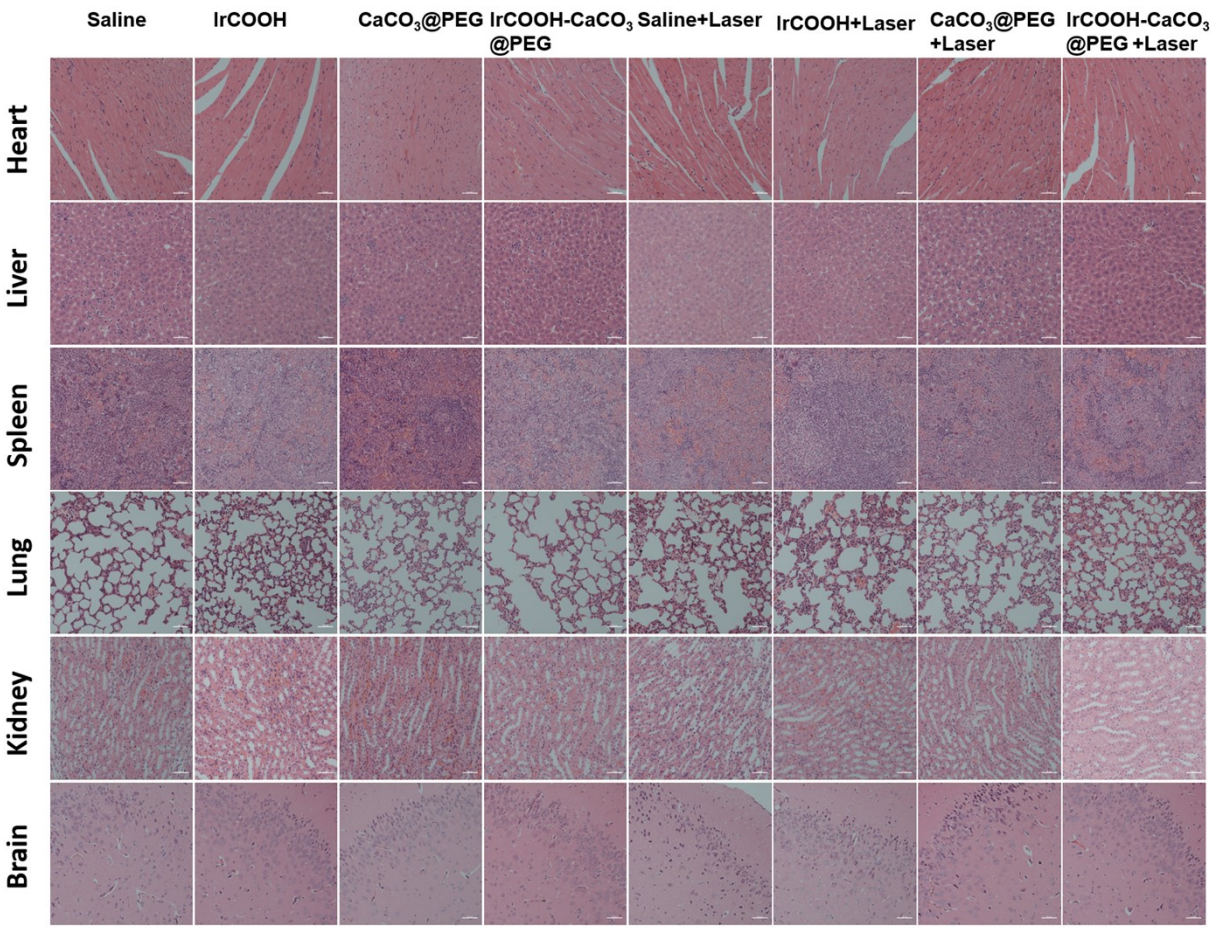

Figure S24. Histopathologic slices of the major organs (heart, liver, spleen, lung, kidney, and brain) of 4T1 tumor-bearing mice which were stained with hematoxylin and eosin staining after different treatments.

Table S1. The Ir(III) complexes loading yield.

	Ca (ppb)	Ir (ppb)	Loading yield
Ir1-$CaCO_3$	1124.1±27.8	1.28±0.02	1.2%
IrOH-$CaCO_3$	1647.1±12.8	1.13±0.06	0.7%
IrCOOH-$CaCO_3$	1443.3±10.4	14.90±1.29	15.6%

The Ca was measured by ICP-OES, while the Ir was measured by ICP-MS.

Table S2. Hydrodynamic diameter and polydispersity determined by dynamic light scattering.

Sample	Diameter (nm)	Polydispersity
Ir1	/	/
IrOH	/	/
IrCOOH	/	/
$CaCO_3$	126.73±0.65	0.100±0.019
Ir1- $CaCO_3$	136.17±0.83	0.116±0.029
IrOH- $CaCO_3$	137.16±1.38	0.125±0.016
IrCOOH-$CaCO_3$	168.76±3.73	0.169±0.014
IrCOOH-$CaCO_3$@PEG	188.75±3.79	0.196±0.030